*Molecular Vision* 2017; 23:90-102 <http://www.molvis.org/molvis/v23/90>
Received 18 August 2016 | Accepted 6 March 2017 | Published 8 March 2017



# Reduced phosphoCREB in Müller glia during retinal degeneration in *rd10* mice

**Enheng Dong,[1] Amelia Bachleda,[2] Yubin Xiong,[1] Shoji Osawa,[1] Ellen R. Weiss[1,2,3]**

**(The first two authors contributed equally to this study.)**

*[1]Department of Cell Biology and Physiology, The University of North Carolina at Chapel Hill, NC; [2]The Neuroscience Center, The University of North Carolina at Chapel Hill, NC; [3]The Lineberger Comprehensive Cancer Center, The University of North Carolina at Chapel Hill, NC*

**Purpose:** The mechanisms that trigger retinal degeneration are not well understood, despite the availability of several animal models with different mutations. In the present report, the *rd10* mouse, a model for retinitis pigmentosa (RP) that contains a mutation in the gene for PDE6β (*Pde6b*), is used to evaluate gliosis, as a marker for retinal stress, and cyclic AMP response element binding protein (CREB) phosphorylation, which may be important early in retinal degeneration.
**Methods:** Wild-type C57Bl6J and *rd10* mice raised under cyclic light were examined for changes in gliosis and CREB phosphorylation for approximately 3 weeks beginning at P14 to P17 using immunocytochemistry. Mice raised under normal cyclic light and in complete darkness were also compared for changes in CREB phosphorylation.
**Results:** Gliosis in *rd10* mice raised under cyclic light was apparent at P17, before extensive degeneration of the photoreceptor layer is visible, and increased over time. Phosphorylation of CREB at Ser133 (pCREB) was detected in Müller glia (MG) in the wild-type and *rd10* mice. However, at all phases of photoreceptor degeneration, the pCREB levels were lower in the *rd10* mice. We also observed extensive migration of MG cell bodies to the outer nuclear layer (ONL) during degeneration. In contrast to the mice raised under cyclic light, the *rd10* mice raised in the dark exhibited slower rates of degeneration. When the dark-reared mice were exposed to cyclic light, the photoreceptor layer degenerated within 4 days to approximately one to two rows of nuclei. Interestingly, the pCREB levels in the MG also decreased during this 4-day cyclic light exposure compared to the levels in the *rd10* mice raised continuously in the dark.
**Conclusions:** The results of these studies suggest that photoreceptors communicate directly or indirectly with MG at early stages, inducing gliosis before extensive retinal degeneration is apparent in *rd10* mice. Surprisingly, phosphorylation of CREB is downregulated in the MG. These results raise the interesting possibility that Müller glia undergo CREB-mediated transcriptional changes that influence photoreceptor degeneration either positively or negatively. Unlike canine models of RP, no increase in pCREB was observed in photoreceptor cells during this period suggesting possible mechanistic differences in the role of CREB in photoreceptors between these species.

Retinitis pigmentosa (RP) is a class of retinopathies typically characterized by rod photoreceptor degeneration followed by cone degeneration and leads, in most cases, to total blindness. Approximately 4% to 5% of patients with recessive RP have mutations in the genes for PDE6α, and 3% to 4% have mutations in PDE6β, the catalytic subunits of cGMP-phosphodiesterase 6 (PDE6) [1,2]. The study of mouse models with mutations in orthologous proteins provides information on the critical factors that cause RP in humans. In rods, PDE6 is composed of catalytic α and β subunits and two inhibitory γ subunits. Light-activated rhodopsin stimulates the activation of its G protein, transducin ($G_t$), which activates PDE6 by the binding of the inhibitory PDE6γ subunits to $G_t\alpha$. The breakdown of cGMP catalyzed by activated PDE6 leads to closure of the cGMP-gated ion channels and hyperpolarization of rod photoreceptors [3]. These events are the initial steps in phototransduction. The *rd10* mouse possesses a mutation in the *pde6β* gene that reduces the level of this enzyme and results in a retinal degeneration phenotype [4]. In *rd10* mice, degeneration begins at approximately P17–20 [4-6]. This timing makes it possible to distinguish biochemical and transcriptional events that are involved early in retinal degeneration from those that occur during normal postnatal retinal development.

The principal glial cells in the retina are the Müller glia (MG), which support the survival and function of the neuronal population through various mechanisms, including playing a protective role in response to retinopathic insults [7]. Thus, MG are highly sensitive to genetic and environmental stress

Correspondence to: Ellen R. Weiss, The University of North Carolina at Chapel Hill, Department of Cell Biology and Physiology, 5340B MBRB, Chapel Hill, NC 27599; Phone: (919) 966-7683; FAX: (919) 966-6927; email: erweiss@med.unc.edu
Dr. Amelia Bachleda is now at: The Institute for Learning and Brain Sciences, University of Washington, Seattle, WA 98195.
Dr. Enheng Dong is now at: The School of Public Health, Xinxiang Medical University, Xinxiang City, Henan Province, China 453003.

in neurons and to physical damage (e.g., diabetic retinopathy, proliferative retinopathies, retinitis pigmentosa, and retinal detachment) [7-10]. These conditions result in disruption of multiple functions of the MG, including $K^+$ homeostasis in the extracellular environment, ammonia detoxification, and glutamate recycling. MG also undergo reactive gliosis, manifested as increased expression of intermediate filaments, such as glial fibrillary acidic protein (GFAP) and vimentin, hypertrophy, and the secretion of cytokines and neurotrophic factors [7].

Cyclic AMP response element binding protein (CREB) is a ubiquitous nuclear factor that assembles protein complexes to initiate gene transcription when phosphorylated on Ser133 (pCREB) [11]. CREB is known to play a protective role against degeneration in the central nervous system [12]. In several canine RP models with photoreceptor-specific mutations in genes, a dramatic upregulation of pCREB is observed in photoreceptor cells during degeneration [13]. Therefore, we evaluated the phosphorylation of CREB on Ser133 (pCREB) during photoreceptor degeneration in the *rd10* mice to determine whether CREB might be activated and could play a role in either inhibiting or enhancing retinal degeneration. In contrast to the results reported in similar canine models of RP, we did not observe pCREB in the photoreceptor cells in the *rd10* mice. The difference between canine and mouse models for RP illustrates species variation, although the mutations are in the same proteins, possibly due to different rates of degeneration or mechanistic differences in the photoreceptor degeneration process. Defining the mechanisms behind these species-specific differences may contribute to a better understanding of RP.

In the wild-type and *rd10* retinas, we detected pCREB consistently in the inner nuclear and ganglion cell layers. However, in the *rd10* retinas, the pCREB levels were lower in the MG compared to the MG in the wild-type retinas. The lower pCREB levels were observed before and during the migration of the MG cell bodies toward the outer nuclear layer (ONL), a known response of gliotic MG in the *rd10* retina [14]. The levels of pCREB in the MG were also found to be influenced by light in the *rd10* mouse. Because light is an exacerbating factor for retinal degeneration in this model, these data suggest the intriguing possibility that transcriptional regulation by CREB in MG is affected by light and influences the progress of retinal degeneration.

## METHODS

*Antibodies and reagents:* The antibodies used in this study were purchased from companies listed in Table 1 (primary antibodies) and Table 2 (secondary antibodies). Anti-pCREB was purchased from Cell Signaling (Danvers, MA) as either an unconjugated antibody (anti-pCREB; catalog #9198) or as a conjugate to Alexa Fluor 488 (anti-pCREB- Alexa Fluor 488 conjugate; catalog #9187; see Table 1). Two antibodies were directly conjugated to florescent dyes in our laboratory as follows. The antibody for SOX9 (#AB5535; Millipore; Billerica, MA) was conjugated to CF555 by diluting it 1:2 with the Mix-n-Stain CF555 antibody labeling kit (Biotium, Inc.; Hayward, CA) according to the manufacturer's directions. Similarly, Iba1 (#019–19741; Wako Chemicals USA, Inc.; Richmond, VA) was conjugated to CF488A by diluting it 1:2 using the Mix-n-Stain CF488A kit from the same company. Hoechst33258 was purchased from ThermoFisher Scientific Inc. (Pittsburgh, PA). ProLong Gold antifade mounting media containing 4',6-diamidino-2-phenylindole (DAPI) was purchased from ThermoFisher Scientific Inc. λ-phosphatase was purchased from New England Biolabs (Ipswich, MA).

*Mice:* Wild-type and *rd10* mice on a C57BL/6J background were obtained from Jackson Laboratories (Bar Harbor, MA). The age-matched wild-type and *rd10* mice used for the experiments were raised either under a normal 12 h:12 h light-dark cycle or in total darkness as described in the Results. Mice raised in cyclic light were reared on the same shelf to match the light exposure in the cages as closely as possible.

Table 1. Primary antibodies.

| Antigen | Antibody type | Catalog number | Company |
|---|---|---|---|
| SOX9 | rabbit polyclonal | AB5535 | Millipore (Billerica, MA) |
| SOX2 | mouse monoclonal | MAB2018 | R&D Systems (Minneapolis, MN) |
| GFAP | rabbit polyclonal | Z0334 | DAKO (Carpinteria, CA) |
| pCREB (Ser133) | rabbit monoclonal (87G3) | 9198 | Cell Signaling (Danvers, MA) |
| pCREB (Ser133) | rabbit monoclonal (87G3) | 9187(anti-pCREB-AlexaFluor 488 conjugate) | Cell Signaling (Danvers, MA) |
| CREB | mouse monoclonal (86B10) | 9104 | Cell Signaling (Danvers, MA) |
| Iba1 | rabbit polyclonal | 019–19741 | Wako Chemicals USA, Inc. (Richmond, VA) |

Table 2. Secondary antibodies.

| Antibody | Catalog number | Company |
|---|---|---|
| AlexaFluor 555 goat anti-rabbit IgG | A27039 | ThermoFisher Scientific (Pittsburgh, PA) |
| AlexaFluor 488 goat anti-mouse IgG | A-11001 | |
| AlexaFluor 488 goat anti-rabbit IgG | A-11008 | |
| AlexaFluor 546 goat anti-mouse IgG | A-11003 | |

*Immunocytochemical analysis:* Mice raised in cyclic light were euthanized under ambient white light, and dark-raised animals were euthanized under red light (LED with a peak wavelength at 660 nm ± 20 nm, LEDtronics, Inc., Torrance, CA) by cervical dislocation following procedures in compliance with the Institutional Animal Care and Use Committee at the University of North Carolina at Chapel Hill and in adherence to the ARVO Statement for Use of Animals in Research. Euthanasia was performed between 13:00 and 15:00 to avoid any influence of the time of day. The eyes were enucleated and incubated in 4% paraformaldehyde (PFA) in PBS (1X: 137 mM NaCl, 2.7 mM KCl, 1 mM $Na_2HPO_4$, 1.5 mM $KH_2PO_4$, pH 7.2) for 1 h, followed by removal of the anterior segment and lens in HEPES-Ringer buffer containing 10 mM HEPES, pH 7.5, 120 mM sodium chloride, 0.5 mM potassium chloride, 0.2 mM calcium chloride, 0.2 mM magnesium chloride, 0.1 mM EDTA, 10 mM glucose, and 1 mM dithiothreitol (DTT). The eyecups were incubated with 4% paraformaldehyde (PFA) in PBS overnight at 4 °C, washed five times with PBS, and equilibrated sequentially in 10%, 20%, and 30% sucrose in PBS, followed by embedding in optimum cutting temperature compound (OCT) and freezing at −80 °C. The eyecups were cryosectioned at 12-µm thickness at −20 °C and stored at −80 °C until used for immunocytochemistry. For all imaging and quantification in Figure 1, Figure 2, Figure 3, Figure 4, and Figure 5 (with the exception of the image of the P34 mice shown in Figure 4B), the regions of the retina adjacent to the optic nerve were selected to ensure reproducibility across experiments.

For GFAP and SOX2 costaining (Figure 1), the cryostat sections were blocked in PBS containing 10% goat serum and 1.0% Triton X-100 for 2 h. The sections were incubated overnight with a polyclonal antibody against GFAP at 1:500 and a monoclonal antibody against SOX2 at 1:100 in PBS containing 5% goat serum and 0.1% Triton-X-100 at 4 °C. After three washes in PBS, the samples were incubated with Alexa Fluor 488 goat anti-rabbit immunoglobulin (IgG; 1:2,000) and Alexa Fluor 546 goat anti-mouse IgG (1:1,000) for 1 h at room temperature in the same buffer as the primary antibody incubation. After two washes in PBS, the samples were incubated for 5 min in Hoechst33258 at 1:10,000 to stain the nuclei, followed by an additional three washes in PBS. A Zeiss LSM710 microscope (Carl Zeiss Microscopy, Thornwood, NY) was used to collect Z-stacks at 20X, which were processed as maximum projections using the computer program, Adobe Photoshop (Adobe Systems Incorporated, San José, CA).

For immunostaining with CREB, pCREB, SOX9, and Iba1 antibodies (Figure 2, Figure 3, Figure 4, and Figure 5), the slides were placed at room temperature overnight to enhance the attachment of the sections to the slides. These slides were incubated in PBS for 5 min, incubated in blocking buffer (PBS containing 0.5% Triton X-100 and 5% normal goat serum) for 1–2 h and then incubated overnight at 4 °C in PBS containing 0.5% Triton X-100 and primary antibody at concentrations indicated in the figure legends. After washing five times with PBS, the sections were stained with the anti-pCREB antibody 87G3 and the anti-CREB antibody 86B10 followed by incubating with secondary antibodies, Alexa Fluor 555 goat anti-rabbit IgG and Alexa Fluor 488 goat anti-mouse IgG at 1:1,000 at room temperature for 2 h (Figure 2B). The secondary antibody step was eliminated when the sections were costained for pCREB and SOX9 (Figure 3 and Figure 5) because the antibodies were directly conjugated to fluorophores 488A (anti-pCREB-Alexa Fluor 488 conjugate from Cell Signaling; see Table 1) and CF555 (by us, using the Mix-n-Stain CF555 antibody labeling kit from Biotium; see above), respectively. The sections were then rinsed five times in PBS and covered with ProLong Gold antifade mounting media containing DAPI to stain the nuclei. Images were collected using either an Olympus FV1000 (Olympus America, Center Valley, PA) or a Zeiss 880 confocal microscope. Under the Olympus confocal microscope, the samples were excited with the 405 nm diode laser, the 488 nm spectral line of the Argon ion laser, and the 543 nm helium-neon laser to acquire fluorescence. A series of z-stacks was acquired with an Olympus PLAPON 60x/1.42 objective in sequential mode to avoid bleed-through (Figure 2B and Figure 5). Under the Zeiss confocal microscope, the samples were excited with a 405 diode laser, the 488 nm spectral line of an Argon-ion laser, and a 561 nm-Helium Neon laser to acquire

fluorescence. Z-stacks were acquired with a Zeiss Plan-Apo 63x oil/1.4 objective in sequential mode (Figure 3 and Figure 4).

To validate the specificity of the anti-pCREB antibody for the phosphorylated form of this transcription factor (Figure 2A), slides containing wild-type mouse sections were preincubated for 10 min in PBS containing 0.3% Triton-X-100 and 1% bovine serum albumin (BSA). The slides were rinsed three times in PBS followed by incubation with or without 3,000 units of λ-phosphatase for 2 h at 37 °C in 250 µl buffer supplied by the manufacturer. The slides were subsequently rinsed five times in PBS and stained for pCREB with anti-pCREB-Alexa Fluor 488 conjugate. Z-stacks were acquired on a Zeiss microscope as described above.

*Statistical analysis:* For quantification of pCREB staining in the MG compared to other cells in the wild-type and *rd10* retinas (Figure 3 and Figure 5), individual z-stack images were selected and converted to RGB TIFF files. The pixel

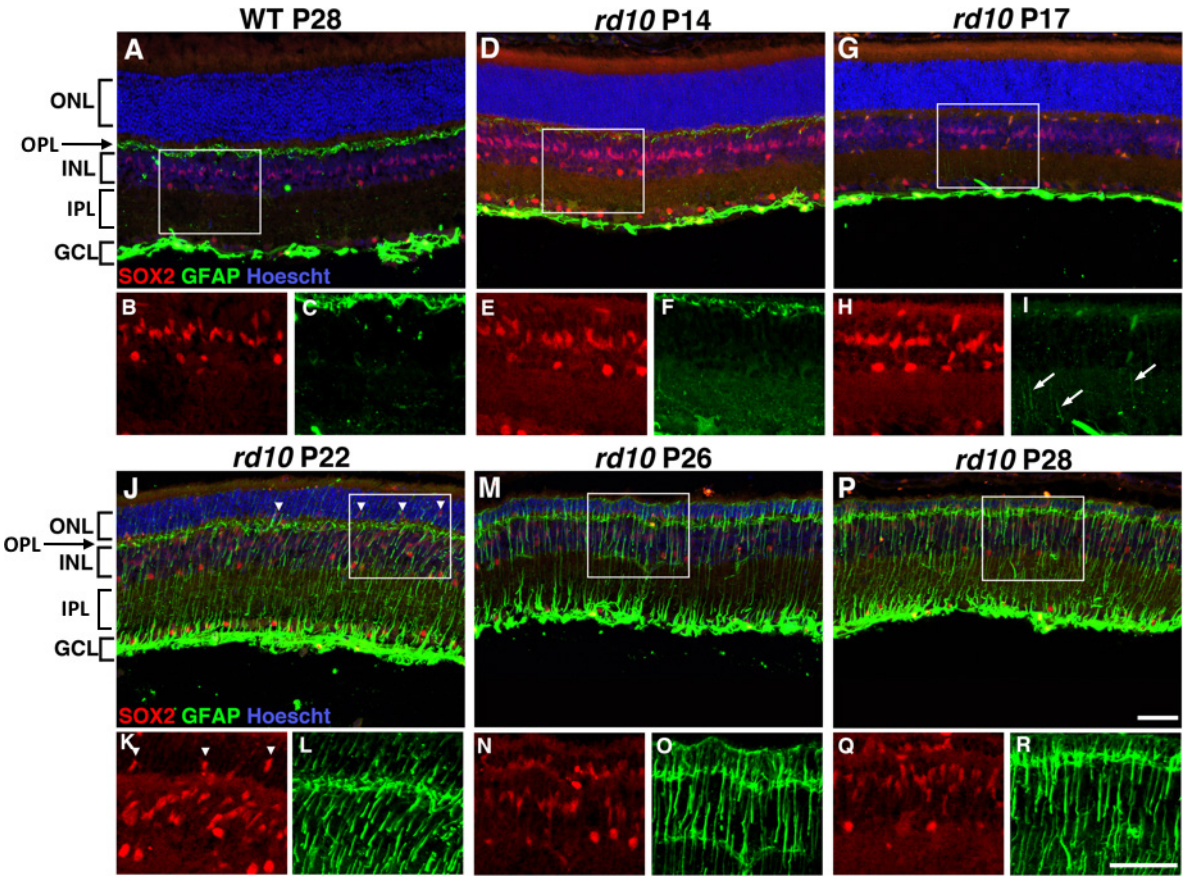


Figure 1. Gliosis occurs early in retinal degeneration in *rd10* retinas. **A**: Wild type C57BL/6J mice at P28. **B**, **C**: enlargement of the insert in **A** showing SOX2 staining (red) in Müller glia and GFAP staining (green), respectively. GFAP staining is observed in astrocytes and in the MG end feet within the nerve fiber layer at the inner retinal border with the vitreous space, but do not exhibit typical glial scarring in the inner retina (**C**) that is characteristic of retinal degeneration. **D**: *rd10* mice at P14. **E**, **F**: enlargement of the insert in **D** showing SOX2 staining (red) in Müller glia and GFAP staining (green), respectively. The *rd10* mice appear similar to wild-type mice in **A** with no obvious gliosis (**F**). **G**: rd10 at P17. **H**, **I**: enlargement of the insert in **G** showing SOX2 staining (red) in Müller glia and GFAP staining (green), respectively. At P17, GFAP expression MG initially appears as longitudinal streaks in the IPL, which is a marker for gliosis (white arrows; **I**) and increases at **J** (P22), **M** (P26) and **P** (P28). **K**, **L**: enlargement of the insert in **J** showing SOX2 staining (red) in Müller glia and GFAP staining (green), respectively. **N**, **O**: enlargement of the insert in **M** showing SOX2 staining (red) in Müller glia and GFAP staining (green), respectively. **Q**, **R**: enlargement of the insert in **P** showing SOX2 staining (red) in Müller glia and GFAP staining (green), respectively. Staining of MG with the SOX2 antibody also shows the migration of these cell bodies from the INL to the ONL beginning on P22 (**J**, **K**; white arrowheads). These data are representative of 3 experiments on 3 different sets of mice. Anti-GFAP, 1:500; anti-SOX2, 1:100; AlexaFluor488 goat anti-rabbit IgG (1:2000); AlexaFluor 546 goat anti-mouse IgG (1:1,000). The stacks were processed as maximum projections using Zeiss software. ONL, outer nuclear layer; OPL, outer plexiform layer; INL, inner nuclear layer; IPL, inner plexiform layer; GCL, ganglion cell layer; scale bar, 50 µm.

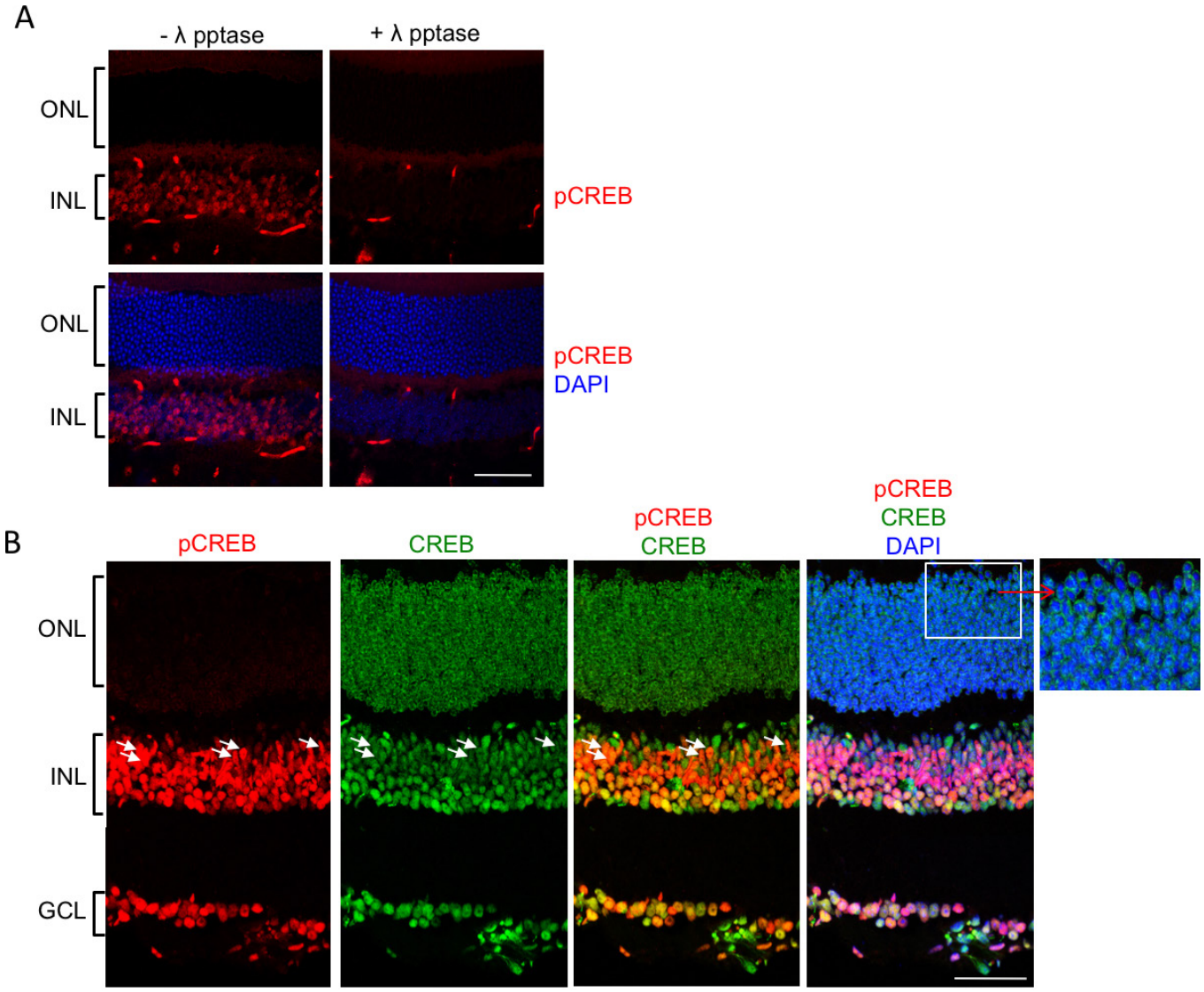


Figure 2. Expression and localization of CREB and pCREB in the wild-type retina at P28. **A**: To verify that phosphorylated cyclic AMP response element binding protein (pCREB) is selectively recognized by the anti-pCREB antibody, wild-type retina sections from mice at P28 were treated without (-) and with (+) λ phosphatase (λ pptase) as described in the Methods, followed by staining with anti-pCREB conjugated to Alexa Fluor 488A (anti-pCREB-Alexa Fluor 488 conjugate; 1:25). pCREB staining was then pseudocolored red using Adobe Photoshop to be consistent with Figure 2B. No staining was detected in the sections treated with λ phosphatase, indicating that the antibody is specific for the phosphorylated form of CREB. **B**: CREB (green) expression is evident in all three nuclear layers. In contrast, pCREB (stained with the unconjugated anti-pCREB antibody followed by secondary antibody; red) is visualized in a subset of cells, including the Müller glia (MG; based on the elongated shape of their cell bodies; white arrows) in the INL as well as other cells in the INL and the GCL. Notably, pCREB is absent from the ONL, which contains the nuclei of the photoreceptors. *Inset*: Magnified view of the ONL; anti-CREB, 1:50; anti-pCREB, 1:200; secondary antibodies Alexa Fluor 488 goat anti-mouse immunoglobulin G (IgG) and Alexa Fluor 555 goat anti-rabbit IgG at 1:1,000. The z-stacks from a single mouse retina were processed as maximum projections using Adobe Photoshop. GCL, ganglion cell layer; INL, inner nuclear layer; ONL, outer nuclear layer. Scale bar = 50 µm.

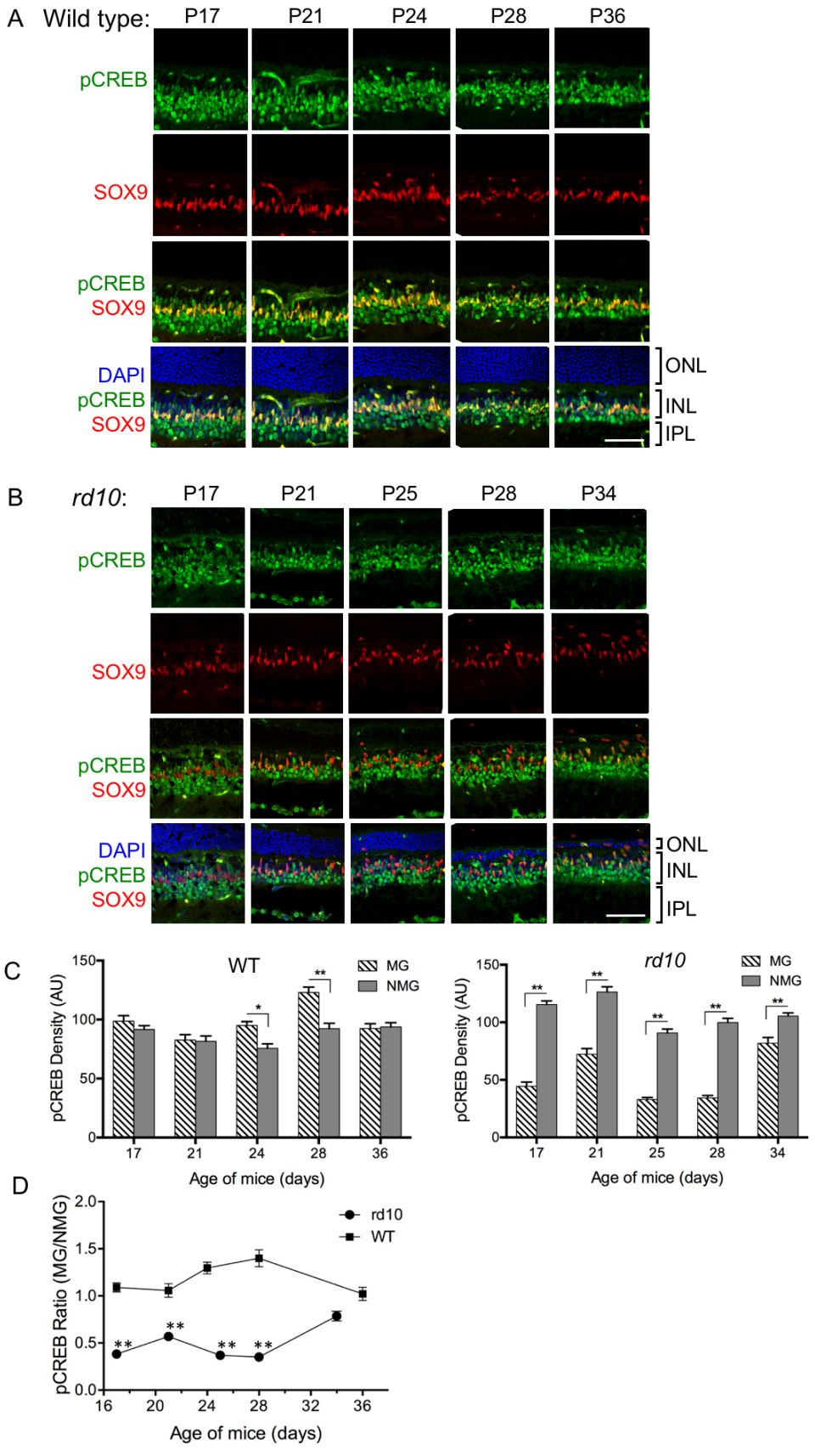


Figure 3. Changes in MG pCREB levels during retinal degeneration. Retinas from wild-type (**A**) and *rd10* (**B**) mice were stained for pCREB (green), SOX9 (red) to label Müller glia (MG) and 4',6-diamidino-2-phenylindole (DAPI; blue) to label the nuclei. **C**: Phospho-CREB levels were quantified in MG and non-Müller glia (NMG) in the retinas from the wild-type and *rd10* mice as described in the Methods. The pCREB levels in MG in the *rd10* mice were lower compared with those in the NMG. In contrast, the pCREB levels were equal to or slightly higher than the levels in NMG in the wild-type mice. **D**: A time course of the ratio of pCREB (MG/NMG) demonstrates that pCREB in the MG is lower at all points in the *rd10* mice compared with the wild-type mice. pCREB appeared to decrease in the *rd10* mice during the progression of retinal degeneration, followed by an increase toward wild-type levels at P34. The data are representative of three separate experiments on two sets of wild-type and three sets of *rd10* mice. The pattern of transient reduction in the pCREB levels in MG was consistent between experiments. Anti-SOX9 conjugated to CF555 (see Methods), final antibody concentration, 1:2,000; anti-pCREB conjugated to Alexa Fluor 488A (anti-pCREB-Alexa Fluor 488 conjugate); final antibody concentration; 1:25. A single z slice is presented for each image. The levels of pCREB were quantified as described in the Methods. Error bars represent the standard error of the mean (SEM). For statistical comparisons, a one-way ANOVA was performed using Sidak's multiple comparisons test in **C**, **D**. *p<0.01; **p<0.0001. Scale bar = 50 µm. Although the pCREB ratio between the *rd10* mice retinas at P34 and the wild-type mice retinas at P36 was statistically significant (p = 0.0144), these data were not included because the trend of the *rd10* data made it difficult to assess what the levels would be on P36. Abbreviations: ONL, outer nuclear layer; INL, inner nuclear layer; IPL, inner plexiform layer.

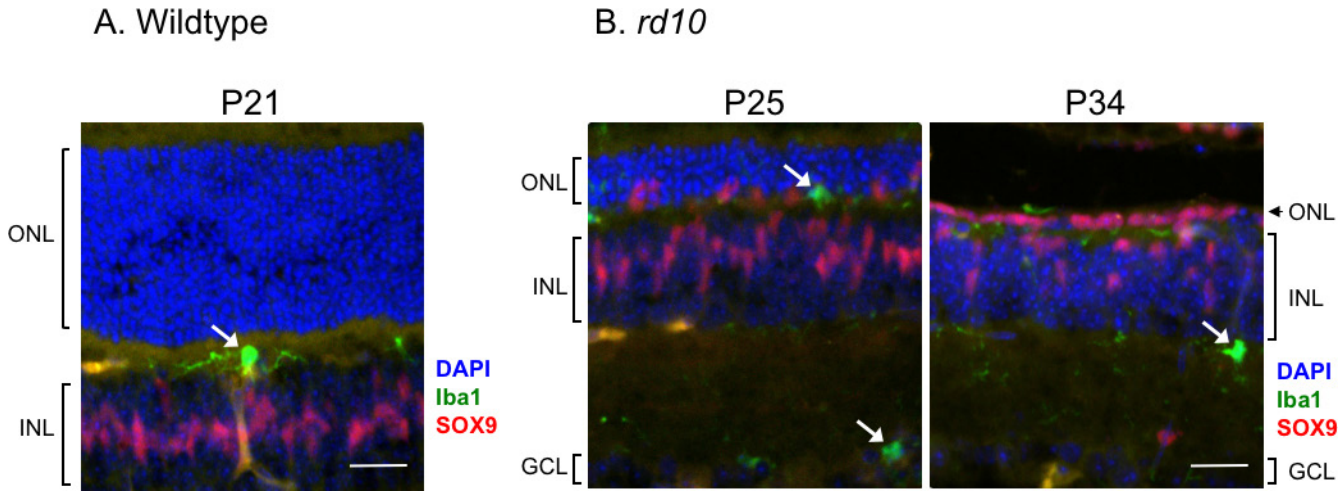


Figure 4. Müller glia and microglia in wild-type and *rd10* retinas. **A**: In wild-type mice, the Müller glia (MG) stained for SOX9 (red) are aligned in the INL. A microglial cell stained with Iba1 (green; marked by white arrow) is shown in the OPL; **B**: In the *rd10* mice, the MG have moved to the inner edge of the ONL by P25. By P34, there are areas where the MG can be observed in a linear array in the ONL, which may be preliminary to the formation of a glial seal (see Discussion). The white arrows indicate microglia. Anti-SOX9 was conjugated to CF555 (see Methods); the final antibody concentration was 1:2,000. The anti-Iba1 was conjugated to CF488A (see Methods); the final antibody concentration was 1:500. A single z slice is presented for each image from a single mouse retina. INL, inner nuclear layer; ONL, outer nuclear layer, GCL, ganglion cell layer. Scale bar = 25 µm.

density of an area of pCREB staining (green) in 20 randomly selected MG cells (identified by SOX9 staining; red) and 20 randomly selected pCREB-positive cells in the inner nuclear layer (INL) that were not MG (non-Müller glia; NMG) was quantified using Fiji (NIH Image, NIH). The ratio of the pCREB staining intensity between the MG and NMG cells ("MG/NMG") was obtained and analyzed using Microsoft Excel (Microsoft, Redmond, WA) and Prism 6 (GraphPad Software, Inc., San Diego, CA). Prism 6 was also used to calculate the standard error of the mean (SEM) and one-way analysis of variance (ANOVA) using Sidak's multiple comparisons test as measures of statistical significance where noted in the figure legends.

## RESULTS

The onset of photoreceptor degeneration in the *rd10* mouse ranges from 17 to 20 days after birth, depending on the study and location in the retina [4-6]. Although a mutation in the *pde6b* gene is the underlying cause, the mechanism that triggers degeneration is unknown. Changes in the retinal gene expression profile in these mice include genes involved in cell survival, apoptosis, and inflammation [6]. Upregulation of GFAP, an intermediate filament protein, has been reported in light-damaged retinas within 24 h [14] and in retinas from *rd10* mice at later stages in degeneration during widespread photoreceptor cell death (P28; [6]), but the timing of early GFAP expression in *rd10* mice has not been analyzed. To determine when MG sense stress from photoreceptors, we examined GFAP expression in retina sections from *rd10* mice of different ages. In the experiment shown in Figure 1, Müller glia ranging from P14 to P28 were costained with an antibody against GFAP and an antibody that recognizes SOX2, a Müller glial and amacrine cell marker [15]. In the wild-type P28 retinas, GFAP staining was observed in the MG end feet and in the astrocytes located in the ganglion cell and nerve fiber layers (Figure 1A) as described previously [16]. In some sections, GFAP staining was also observed in the outer plexiform layer (OPL), which has been described previously, although it is not clear what this staining represents [17,18]. These observations were consistent with reports that, unlike astrocytes, MG do not express significant levels of GFAP under homeostatic conditions [7,19,20]. The MG in the *rd10* retinas at P14 exhibit no difference in GFAP staining compared to the MG in the wild-type retinas (Figure 1F compared to Figure 1C). In contrast, at P17, the typical longitudinal streaks that represent GFAP upregulation associated with gliosis were observed (white arrows in Figure 1I). This is the earliest time at which gliosis has been detected in the *rd10* mouse. By P22, and at later stages of retinal degeneration, GFAP staining in longitudinal streaks was abundant in the *rd10* retinas (Figure 1L,O,R). These results demonstrate that upregulation of GFAP expression occurs at early stages of degeneration before severe loss of photoreceptors, suggesting early communication from the photoreceptors to the MG in response to stress. Migration of MG cells into the ONL was

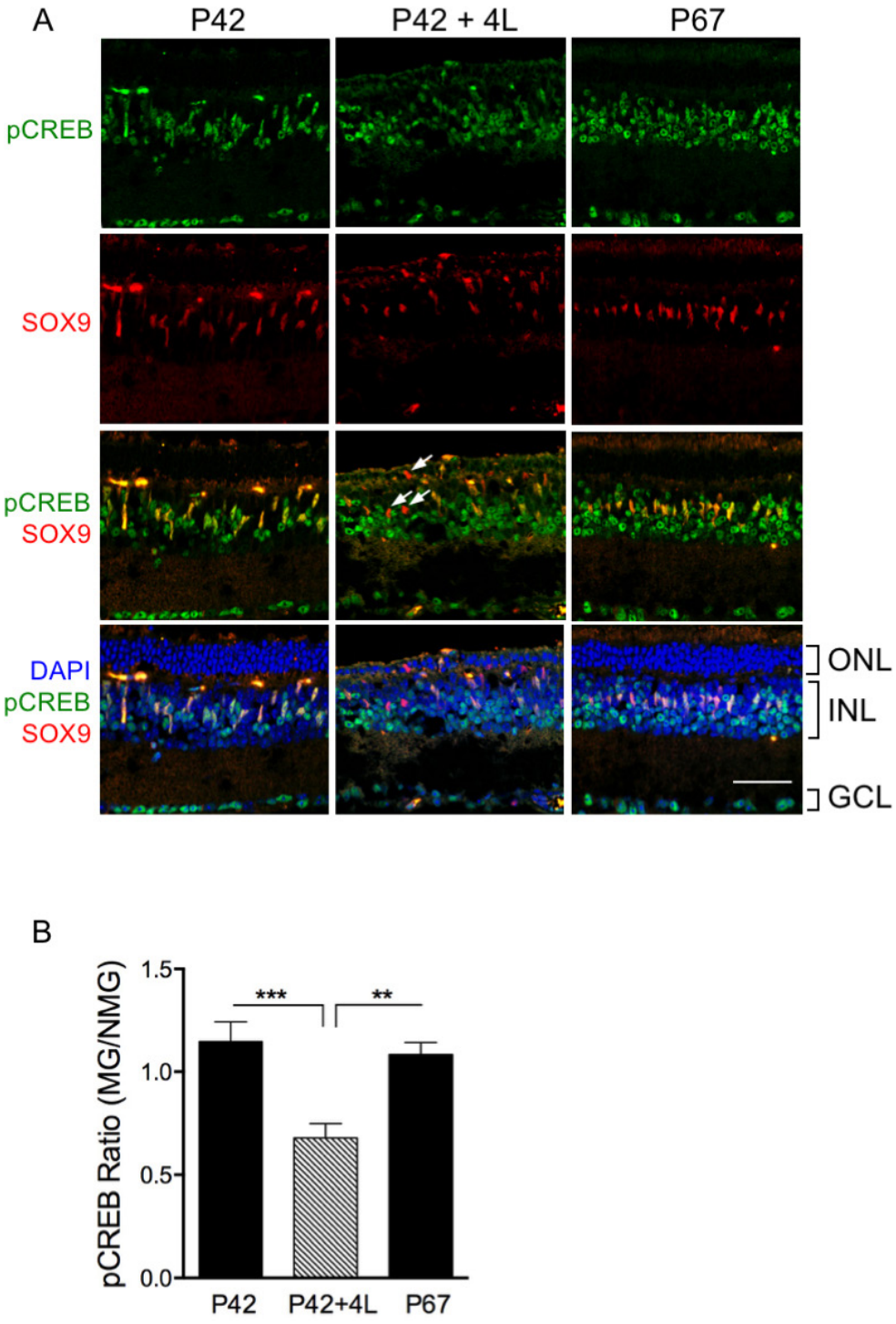


Figure 5. *rd10* retinas from dark-reared mice undergo slower degeneration compared with retinas from cyclic light-reared mice. **A**: At P42 and P67 raised in the dark, a significant number of photoreceptor cell nuclei (stained with 4',6-diamidino-2-phenylindole (DAPI); blue) are still present (five to six rows), based on the thickness of the outer nuclear layer (ONL). Mice placed in normal cyclic light at P42 for 4 days (P42 + 4L) undergo rapid degeneration, such that the ONL is approximately one to two rows of nuclei at the end of day 4. pCREB (green) is detected in many, but not all, of the Müller glia (MG) in the P42 + 4L mice. White arrows, the MG nuclei do not display pCREB staining. **B**: Quantification of the images from the *rd10* mice raised in the dark and then exposed to light (P42 + 4L) demonstrates a general reduction of pCREB in the MG compared with the retinas from the P42 and P67 mice maintained in the dark. Anti-SOX9 conjugated to CF555 (see Methods), final antibody concentration, 1:2,000; anti-pCREB conjugated to Alexa Fluor 488 (anti-pCREB-Alexa Fluor 488 conjugate); final antibody concentration; 1:100. A single z slice is presented for each image. Each image represents a single mouse retina. Error bars represent the standard error of the mean (SEM). Scale bar = 50 µm. **p = 0 .0012; ***p = 0.0002. ONL, outer nuclear layer; INL, inner nuclear layer; GCL, ganglion cell layer.

also observed at P22, as shown by the staining of MG with the anti-SOX2 antibody (white arrowheads; Figure 1J,K).

Because phosphorylation of CREB on Ser133 (pCREB) is detected in photoreceptors in mid to late stages of degeneration in canine models of RP, including those with mutations in the PDE6β subunit (e.g., rcd1 in [13]), we were interested in comparing the cellular locations of CREB and pCREB in wild-type mouse retinas with immunocytochemistry. First, to determine that the anti-pCREB antibody is specific, slides of wild-type retinas were treated with λ phosphatase before staining (Figure 2A). The results demonstrate the presence of pCREB staining in the INL in the absence of phosphatase (- λ pptase). However, pCREB staining was absent when the slides were pretreated with the phosphatase (+ λ pptase). Therefore, the anti-pCREB antibody specifically recognized the phosphorylated form of CREB (pCREB). In the wild-type mice, CREB was expressed in most of the cells in the three nuclear layers of the retina (Figure 2B). pCREB was detected in a subset of cells, including Müller glia, based on the elongated shape of their cell bodies (white arrows) but was notably absent from photoreceptor cells (the ONL), as seen in Figure 2A and in the inset of Figure 2B.

Based on reports that CREB activity can perform an antiapoptotic function in retinas undergoing stress [21], pCREB levels were compared in wild-type (Figure 3A) and *rd10* (Figure 3B) mouse retinas over approximately 3 weeks beginning at P17, a period during which progressively greater degeneration of the photoreceptor layer was visible, based on the thickness of the ONL (Figure 3B). An antibody to SOX9, a transcription factor expressed exclusively in MG in the adult retina [22], was used to localize the MG cell bodies. The MG in the wild-type retinas were colabeled for SOX9 and pCREB, confirming that CREB is phosphorylated in MG. The wild-type and *rd10* retinas were examined at P17 when GFAP staining first became apparent in *rd10* mice (Figure 1I). pCREB also colocalized with SOX9 in the MG in the *rd10* mouse retinas. Based on quantitative analysis (Figure 3C), the levels of pCREB appeared to be similar between MG and non-Müller glia (NMG) in the wild-type retinas. However, in the *rd10* retinas, pCREB was statistically significantly reduced in the MG compared with the NMG. When the ratio of staining for pCREB in MG/NMG was compared for the retinas from the two mouse lines, it is clear that the pCREB levels were statistically significantly lower in the *rd10* mice compared with the wild-type mice until later stages of degeneration (approximately P34) when the levels of pCREB in *rd10* mice appeared to increase toward wild-type levels (Figure 3D).

Interestingly, pCREB increased statistically significantly in photoreceptors in the *rcd1* canine model at midstages of degeneration [13]. In the present studies, faint pCREB staining was occasionally, but not consistently, observed in the ONL at later stages of degeneration (P34) in the *rd10* mice, when the ONL was composed of one to two rows of nuclei. These cells are not likely to be MG based on their shape and lack of SOX9 staining (data not shown). According to previous reports describing the time course of photoreceptor degeneration in *rd10* mice, these cells are likely to be cones [5,6]. At P25 (Figure 4B), the MG (stained with SOX9; red) were observed to enter the ONL in the *rd10* retinas. They appeared to form a partial barrier between the single layer of photoreceptor nuclei and the region where the RPE and the choroid are located (P34; Figure 4B). Recently, microglia have been identified in patients with RP and in mouse models for RP [2,23,24]. Therefore, we stained sections with an antibody to Iba1 (green) to determine whether microglia are located in the ONL. In Figure 4B, the ONL cells are identified as MG rather than microglia based on the presence of SOX9. Microglia cell bodies can be found throughout the inner nuclear and outer plexiform layers (white arrows) in the wild-type (Figure 4A) and *rd10* (Figure 4B) retinas, based on Iba1 staining. Some small extensions of microglia processes were visible adjacent to the MG in the ONL at P34.

It has been reported that *rd10* mice undergo more rapid degeneration when they are raised under normal cyclic light compared with mice raised in the dark [4,25]. Similarly, several inherited retinopathies in humans are exacerbated by light [26]. Therefore, we examined the levels of pCREB and the thickness of the ONL in the dark-reared *rd10* mice at P42 and P67 (Figure 5). Compared with the cyclic light-reared *rd10* mice at P34 (Figure 3B and Figure 4B), the ONL at P42 in the dark-reared mice was significantly thicker (Figure 5A; P42), similar to P28 or earlier in *rd10* mice raised in cyclic light (Figure 3B). The ONL persisted even at P67 with at least four to five rows of nuclei. In contrast, when the 42-day-old dark-reared mice were placed in ambient cyclic light for 4 days (Figure 5A; P42+4L), there was a rapid degeneration such that the ONL was reduced to one to two rows of nuclei. Interestingly, in these mice, MG that did not express pCREB were detected (Figure 5A; P42+L, white arrows), and the pCREB levels were statistically significantly lower in these mice than in the dark-adapted animals (Figure 5B). These observations are consistent with the results in Figure 3 and indicate that light exposure, rather than simply age, appears to play an important role in the levels of transcription mediated by pCREB and in disease progression. In addition, during the 4-day light exposure, the MG cell bodies became disorganized and began to move into the ONL. In contrast, the

MG in the dark-reared animals at P67 were still located in the INL (Figure 5A). These intriguing differences demonstrate the critical importance of light to transcriptional regulation in MG and the overall phenotype of the *rd10* mouse.

## DISCUSSION

Müller glia are critical for the proper development, structure, and function of the mature retina [7,10]. In response to genetic and environmental insults to the retina, MG initiate a stress response (gliosis), in which intermediate filaments, such as GFAP and vimentin, are upregulated [7]. In the present study, we report that increased expression of GFAP in MG occurs as early as P17 in *rd10* mice, which is before photoreceptor loss becomes severe. This result indicates for the first time that early communication of stress signals occurs between photoreceptors and MG and introduces the question of how interactions between photoreceptors and MG influence the degeneration process. Although it is not clear what signals are transmitted, the upregulation of GFAP in MG during retinal degeneration is part of the remodeling of the retina that occurs alongside neuroplastic changes during degeneration from multiple causes [27]. During remodeling, as described by Marc and Strettoi [27], MG cell bodies move toward the ONL. Gliosis is upregulated at this time. We observed MG migrating into the ONL at P22-P25 (Figure 1 and Figure 4). In some parts of the ONL, these cells appear to fill the spaces left by degenerating photoreceptors (P34; Figure 4). This activity is likely to be preliminary to the formation of a glial seal, which is thought to be triggered by cone loss and occurs later in the remodeling process in mice undergoing RP [28].

CREB is one of the transcription factors implicated in neuronal survival, as well as playing a key role in memory formation and plasticity in the central nervous system [12]. In the present study, we observed a statistically significant reduction in phosphorylation of CREB in the MG during degeneration in the *rd10* mice. Reduced pCREB also coincided with the movement of MG cell bodies toward the ONL in these experiments. There are approximately 4,000 target sites for CREB in the human genome [29]. Therefore, identifying the changes in gene expression that result from decreased CREB activity is a challenging task but one that is likely to lead to important information regarding transcriptional events that are part of the retinal degeneration process. Western blot analysis has shown an approximately 30% decline in pCREB at P11 in *rd1* mice [30], which is when photoreceptor degeneration begins in that animal model. However, in those studies, the cells in which this decline occurred were not identified. We also observed that pCREB levels appear to slowly increase toward wild-type levels in MG in the *rd10* mouse by P34 (Figure 3C), at which time rod photoreceptor degeneration is reported to be complete, leaving only cones [5,6]. Although we did not define how pCREB levels are regulated in the present study, reports have suggested that factors, such as brain derived neurotrophic factor (BDNF), ciliary neurotrophic factor (CNTF), and fibroblast growth factor 2 (FGF2), can stimulate CREB phosphorylation in MG under various in vitro and in vivo conditions [31-34]. In addition, in developing chick embryo explants and in adult chickens, glutamate indirectly stimulates CREB phosphorylation in MG, which may occur through the NO/guanylyl cyclase/protein kinase G pathway [35].

Recent work by Harada et al. [34] revealed a critical role for BDNF in MG via the TrkB receptor in preventing or slowing photoreceptor loss upon exposure to *N*-methyl-*N*-nitrosourea (MNU). In wild-type mice, intraocular injection of BDNF increases pCREB levels in MG. However, this increase is prevented in mice in which TrkB is conditionally ablated from MG cells, resulting in a disruption of neurotrophic factor production downstream from BDNF/TrkB and implicating MG in the paracrine regulation of photoreceptor stability via pCREB-mediated transcriptional events. It is possible that signaling from the photoreceptors directly or indirectly downregulates TrkB signaling, by reducing the levels of BDNF in the *rd10* retinas, reducing the TrkB levels, or interfering with events downstream of TrkB. Interestingly, Hanif et al. demonstrated that injection of a TrkB antagonist inhibits exercise-induced delay of retinal degeneration in *rd10* mice [36]. It will be important to determine whether communication of photoreceptor degeneration to the MG and the subsequent changes in the pCREB levels in the MG act as an attempt to rescue photoreceptors or accelerate their degeneration.

Dark-reared *rd10* retinas were observed to degenerate more slowly than those raised under cyclic light as previously reported [4]. Exposure of a dark-reared 42-day-old mouse to ambient cyclic light for 4 days resulted in rapid degeneration, with an ONL thickness that was approximately equivalent to P28 in light-reared mouse retinas (Figure 5). Therefore, this change in degeneration kinetics is directly correlated with exposure to light. The prevailing theory in humans and mice with PDE mutations (such as the *rd10* mouse) is that a continuous flow of cations through the cGMP-gated ion channels directly induces retinal degeneration [1]. However, if that were the case, one might expect that dark-reared wild-type mice would exhibit accelerated retinal degeneration. In fact, just the opposite appears to be true (Figure 5) [4, 25]. It has also been reported that rod $G_t\alpha$ knockout ($Gnat1^{-/-}$) mice display slow degeneration, although this mouse should mimic

the dark-adapted retina where cGMP levels are high and the ion channels are maintained in an open state. Therefore, the cause of retinal degeneration in humans and animals with defective PDE6 activity is likely to be significantly more complex.

Finally, previous work in canine animals with mutations in the PDE6β gene (*rcd1*), and in other canine genetic models of RP, such as *rcd2*, *erd*, *prcd*, and *T4RHO*, demonstrated that phosphorylated CREB is dramatically upregulated in photoreceptors with no obvious indication of changes in pCREB in the INL [13]. Surprisingly, we did not observe a similar result in the *rd10* mice. In some sections, a barely detectable amount of pCREB appeared to localize to a few photoreceptor cell nuclei at P34, when the ONL was reduced to one or two nuclear layers (data not shown). Based on previous reports, these photoreceptors are likely to be cones [6]. The reason for this apparent difference between canine and mouse models is unclear. Although the naturally occurring *rcd1* canine model of RP the *pde6β* gene [37], the time course of normal and pathogenic development in canine retinas is different from that in mice. It takes approximately 60 days for the canine retina to mature [38], whereas maturation of the mouse retina is considered complete at approximately P30 [39,40]. Abnormal development, characterized by disrupted formation of rod outer segments, is apparent in the canine *rcd1* retina at approximately P13, and degeneration begins at approximately P25 [38]. The loss of rods is complete at 1 year. It is possible that the effect of the mutations in canines may occur at an earlier phase in retinal development, thus altering transcriptional networks in ways that are different from that in *rd10* mice. In addition, canine retinas produce melatonin whereas C57Bl6 mice do not [41,42]. A role for circadian rhythm in these differences cannot absolutely be ruled out, although we were careful to perform our experiments at the same time of the day to eliminate potential differences caused by photoentrainment. Whether the lack of pCREB in photoreceptor cells is also true in other RP mouse models, other animal models, or patients with retinal degeneration remains to be determined.

## ACKNOWLEDGMENTS

NIH grants R01EY012224; R01EY022341. Imaging was supported by the Confocal and Multiphoton Imaging Core of NINDS Center Grant P30NS045892 and by the Hooker Imaging Core, Department of Cell Biology and Physiology. We thank Vladimir Ghukasyan, PhD (The Neuroscience Center) and Robert Currin, PhD (Department of Cell Biology and Physiology) for advice and assistance with confocal imaging. We thank David Courson, PhD and Richard Cheney, PhD for helpful discussions.

## REFERENCES

1. Hartong DT, Berson EL, Dryja TP. Retinitis pigmentosa. Lancet 2006; 368:1795-809. [PMID: 17113430].
2. Yoshida N, Ikeda Y, Notomi S, Ishikawa K, Murakami Y, Hisatomi T, Enaida H, Ishibashi T. Laboratory evidence of sustained chronic inflammatory reaction in retinitis pigmentosa. Ophthalmology 2013; 120:e5-12. [PMID: 22986110].
3. Fain GL, Hardie R, Laughlin SB. Phototransduction and the evolution of photoreceptors. Curr Biol 2010; 20:R114-24. [PMID: 20144772].
4. Chang B, Hawes NL, Pardue MT, German AM, Hurd RE, Davisson MT, Nusinowitz S, Rengarajan K, Boyd AP, Sidney SS, Phillips MJ, Stewart RE, Chaudhury R, Nickerson JM, Heckenlively JR, Boatright JH. Two mouse retinal degenerations caused by missense mutations in the β subunit of rod cGMP phosphodiesterase gene. Vision Res 2007; 47:624-33. [PMID: 17267005].
5. Gargini C, Terzibasi E, Mazzoni F, Strettoi E. Retinal organization in the retinal degeneration 10 (*rd10*) mutant mouse: a morphological and ERG study. J Comp Neurol 2007; 500:222-38. [PMID: 17111372].
6. Samardzija M, Wariwoda H, Imsand C, Huber P, Heynen SR, Gubler A, Grimm C. Activation of survival pathways in the degenerating retina of *rd10* mice. Exp Eye Res 2012; 99:17-26. [PMID: 22546314].
7. Bringmann A, Pannicke T, Grosche J, Francke M, Wiedemann P, Skatchkov SN, Osborne NN, Reichenbach A. Müller cells in the healthy and diseased retina. Prog Retin Eye Res 2006; 25:397-424. [PMID: 16839797].
8. Iandiev I, Uckermann O, Pannicke T, Wurm A, Tenckhoff S, Pietsch UC, Reichenbach A, Wiedemann P, Bringmann A, Uhlmann S. Glial cell reactivity in a porcine model of retinal detachment. Invest Ophthalmol Vis Sci 2006; 47:2161-71. [PMID: 16639028].
9. Reichenbach A, Bringmann A. Müller cells in the diseased retina. In: Reichenbach A, Bringmann A, editors. Müller Cells in the Healthy and Diseased Retina. New York: Springer Science+Business Media, LLC; 2010. p. 215–301.
10. Reichenbach A, Bringmann A. New functions of Müller cells. Glia 2013; 61:651-78. [PMID: 23440929].
11. Sakamoto K, Karelina K, Obrietan K. CREB: a multifaceted regulator of neuronal plasticity and protection. J Neurochem 2011; 116:1-9. [PMID: 21044077].
12. Lonze BE, Ginty DD. Function and regulation of CREB family transcription factors in the nervous system. Neuron 2002; 35:605-23. [PMID: 12194863].
13. Beltran WA, Allore HG, Johnson E, Towle V, Tao W, Acland GM, Aguirre GD, Zeiss CJ. CREB1/ATF1 activation in photoreceptor degeneration and protection. Invest Ophthalmol Vis Sci 2009; 50:5355-63. [PMID: 19643965].

14. Joly S, Pernet V, Samardzija M, Grimm C. Pax6-positive Müller glia cells express cell cycle markers but do not proliferate after photoreceptor injury in the mouse retina. Glia 2011; 59:1033-46. [PMID: 21500284].

15. Karl MO, Reh TA. Regenerative medicine for retinal diseases: activating endogenous repair mechanisms. Trends Mol Med 2010; 16:193-202. [PMID: 20303826].

16. Nolte C, Matyash M, Pivneva T, Schipke CG, Ohlemeyer C, Hanisch UK, Kirchhoff F, Kettenmann H. GFAP promoter-controlled EGFP-expressing transgenic mice: a tool to visualize astrocytes and astrogliosis in living brain tissue. Glia 2001; 33:72-86. [PMID: 11169793].

17. Kuzmanovic M, Dudley VJ, Sarthy VP. GFAP promoter drives Müller cell-specific expression in transgenic mice. Invest Ophthalmol Vis Sci 2003; 44:3606-13. [PMID: 12882814].

18. Lecleire-Collet A, Tessier LH, Massin P, Forster V, Brasseur G, Sahel JA, Picaud S. Advanced glycation end products can induce glial reaction and neuronal degeneration in retinal explants. Br J Ophthalmol 2005; 89:1631-3. [PMID: 16299145].

19. Formichella CR, Abella SK, Sims SM, Cathcart HM, Sappington RM. Astrocyte reactivity: a biomarker for retinal ganglion cell health in retinal neurodegeneration. J Clin Cell Immunol 2014; 5:188-[PMID: 25133067].

20. Eisenfeld AJ, Bunt-Milam AH, Sarthy PV. Müller cell expression of glial fibrillary acidic protein after genetic and experimental photoreceptor degeneration in the rat retina. Invest Ophthalmol Vis Sci 1984; 25:1321-8. [PMID: 6386743].

21. Nakazawa M. Therapy options for retinitis pigmentosa. Expert Opin Orphan Drugs 2014; 2:37-52. .

22. Poché RA, Furuta Y, Chaboissier MC, Schedl A, Behringer RR. Sox9 is expressed in mouse multipotent retinal progenitor cells and functions in Muller glial cell development. J Comp Neurol 2008; 510:237-50. [PMID: 18626943].

23. Gupta N, Brown KE, Milam AH. Activated microglia in human retinitis pigmentosa, late-onset retinal degeneration, and age-related macular degeneration. Exp Eye Res 2003; 76:463-71. [PMID: 12634111].

24. Arroba AI, Alvarez-Lindo N, van Rooijen N, de la Rosa EJ. Microglia-mediated IGF-I neuroprotection in the rd10 mouse model of retinitis pigmentosa. Invest Ophthalmol Vis Sci 2011; 52:9124-30. [PMID: 22039242].

25. Cronin T, Lyubarsky A, Bennett J. Dark-rearing the rd10 mouse: implications for therapy. Adv Exp Med Biol 2012; 723:129-36. [PMID: 22183325].

26. Bramall AN, Wright AF, Jacobson SG, McInnes RR. The genomic, biochemical, and cellular responses of the retina in inherited photoreceptor degenerations and prospects for the treatment of these disorders. Annu Rev Neurosci 2010; 33:441-72. [PMID: 20572772].

27. Marc RE, Jones BW, Watt CB, Strettoi E. Neural remodeling in retinal degeneration. Prog Retin Eye Res 2003; 22:607-55. [PMID: 12892644].

28. Jones BW, Watt CB, Frederick JM, Baehr W, Chen CK, Levine EM, Milam AH, Lavail MM, Marc RE. Retinal remodeling triggered by photoreceptor degenerations. J Comp Neurol 2003; 464:1-16. [PMID: 12866125].

29. Zhang X, Odom DT, Koo SH, Conkright MD, Canettieri G, Best J, Chen H, Jenner R, Herbolsheimer E, Jacobsen E, Kadam S, Ecker JR, Emerson B, Hogenesch JB, Unterman T, Young RA, Montminy M. Genome-wide analysis of cAMP-response element binding protein occupancy, phosphorylation, and target gene activation in human tissues. Proc Natl Acad Sci USA 2005; 102:4459-64. [PMID: 15753290].

30. Paquet-Durand F, Azadi S, Hauck SM, Ueffing M, van Veen T, Ekstrom P. Calpain is activated in degenerating photoreceptors in the *rd1* mouse. J Neurochem 2006; 96:802-14. [PMID: 16405498].

31. Azadi S, Johnson LE, Paquet-Durand F, Perez MT, Zhang Y, Ekstrom PA, van Veen T. CNTF+BDNF treatment and neuroprotective pathways in the rd1 mouse retina. Brain Res 2007; 1129:116-29. [PMID: 17156753].

32. Ghai K, Zelinka C, Fischer AJ. Notch signaling influences neuroprotective and proliferative properties of mature Muller glia. J Neurosci 2010; 30:3101-12. [PMID: 20181607].

33. Wahlin KJ, Campochiaro PA, Zack DJ, Adler R. Neurotrophic factors cause activation of intracellular signaling pathways in Muller cells and other cells of the inner retina, but not photoreceptors. Invest Ophthalmol Vis Sci 2000; 41:927-36. [PMID: 10711715].

34. Harada C, Guo X, Namekata K, Kimura A, Nakamura K, Tanaka K, Parada LF, Harada T. Glia- and neuron-specific functions of TrkB signalling during retinal degeneration and regeneration. Nat Commun 2011; 2:189-[PMID: 21304518].

35. Socodato RE, Magalhaes CR, Paes-de-Carvalho R. Glutamate and nitric oxide modulate ERK and CREB phosphorylation in the avian retina: evidence for direct signaling from neurons to Müller glial cells. J Neurochem 2009; 108:417-29. [PMID: 19012740].

36. Hanif AM, Lawson EC, Prunty M, Gogniat M, Aung MH, Chakraborty R, Boatright JH, Pardue MT. Neuroprotective effects of voluntary exercise in an inherited retinal degeneration mouse model. Invest Ophthalmol Vis Sci 2015; 56:6839-46. [PMID: 26567796].

37. Aquirre G, Farber D, Lolley R, Fletcher RT, Chader GJ. Rod-cone dysplasia in Irish setters: a defect in cyclic GMP metabolism in visual cells. Science 1978; 201:1133-4. [PMID: 210508].

38. Farber DB, Danciger JS, Aguirre G. The β subunit of cyclic GMP phosphodiesterase mRNA is deficient in canine rod-cone dysplasia 1. Neuron 1992; 9:349-56. [PMID: 1323314].

39. Blanks JC, Adinolfi AM, Lolley RN. Synaptogenesis in the photoreceptor terminal of the mouse retina. J Comp Neurol 1974; 156:81-93. [PMID: 4836656].

40. LaVail MM. Kinetics of rod outer segment renewal in the developing mouse retina. J Cell Biol 1973; 58:650-61. [PMID: 4747920].

41. Dinet V, Ansari N, Torres-Farfan C, Korf HW. Clock gene expression in the retina of melatonin-proficient (C3H) and melatonin-deficient (C57BL) mice. J Pineal Res 2007; 42:83-91. [PMID: 17198542].

42. Lavoie J, Rosolen SG, Chalier C, Hebert M. Negative impact of melatonin ingestion on the photopic electroretinogram of dogs. Neurosci Lett 2013; 543:78-83. [PMID: 23562505].

Articles are provided courtesy of Emory University and the Zhongshan Ophthalmic Center, Sun Yat-sen University, P.R. China. The print version of this article was created on 8 March 2017. This reflects all typographical corrections and errata to the article through that date. Details of any changes may be found in the online version of the article.